Effect of transient trapping on hydrogen transport near a blunting crack tip

Y. Charles, Jonathan Mougenot, Monique Gaspérini

Effect of transient trapping on hydrogen transport near a blunting crack tip

Yann CHARLES[1], Jonathan MOUGENOT, Monique GASPERINI

Université Sorbonne Paris Nord, Laboratoire des Sciences des Procédés et des Matériaux, LSPM, CNRS, UPR 3407, F-93430, Villetaneuse, France

Abstract

The paper revisits the way transient trapping is introduced in the literature based on the Sofronis and McMeeking model [1] of hydrogen transport. It is shown that the direct use of the improved formulation made by Krom et al. [2] for transient trapping may lead to non-physical results of hydrogen concentration in case of an insulated system. The use of McNabb and Foster trapping kinetic equation is more relevant, and its ability to model both trap creation and kinetic trapping is investigated on a Small Scale Yielding configuration for the sake of comparison with a reference case from the literature. A parametric study is conducted, exhibiting differences with literature, and emphasizes on the significant effect of trapping kinetics on the hydrogen distribution.

keywords: Hydrogen trapping, Crack tip plasticity, Diffusion, Finite elements, Abaqus

1 Introduction

Structures operating in a hydrogenic environment must be carefully designed to prevent early failures by hydrogen embrittlement. This phenomenon results from complex interactions between hydrogen and the material [3]: hydrogen atoms penetrate and diffuse into the material crystal lattice, interact with microstructural defects (acting as traps) and affect the material properties and the conditions of fracture [4]. Hydrogen transport properties depend on the evolution of traps density. Such evolution is encountered in many applications involving plastic deformation or plasma exposed surfaces [5,6]. Considering hydrogen transport in elastic-plastic material, the finite element approach of initial boundary values problems is widely based on the transport equations proposed by Krom et al. [2], following the pioneering work of Sofronis and McMeeking [1].

In these approaches, the hydrogen concentration is the result of hydrogen diffusion through interstitial lattice sites and hydrogen trapping by the material defects (dislocations induced by plastic straining). A relationship between the evolution of mobile and trapped concentrations has been proposed by McNabb and Foster [7], using a first order kinetic reaction to describe the trapping process [8]. Following Oriani [9], an expression of the trapped hydrogen concentration as function of the mobile hydrogen concentration can be obtained at equilibrium. This assumption is reasonable when trapping is very fast compared to the characteristic times of the other processes involved and was used in [1] to obtain the hydrogen transport equation. This model was applied to a Small Scale Yielding (SSY) configuration, which became a benchmark test case for further theoretical and numerical studies on hydrogen diffusion and trapping [1,2,10-17].

Krom et al. [2] pointed out the need to improve the Sofronis and McMeeking transport model for trap creation as it did not insure a correct hydrogen balance in the case of an insulated

[1] Corresponding author, yann.charles@univ-paris13.fr, tel: (33) 1 49 40 34 61, fax: (33) 1 49 40 39 38

system. To account for the trap creation due to plastic strain, they proposed to add an additional term to the transport equation called "strain rate factor". The effect of that extra term was analyzed on the same SSY configuration to underline the consequences on hydrogen repartition ahead of a crack tip under a mode I loading. This modified equation has been used in various papers based on finite element computations to describe hydrogen transport in mechanically loaded structures using both isotropic and crystal plasticity (see, [18-21]).

Later, Kanayama et al. [16] investigated the effect of transient trapping compared to Oriani's equilibrium on the hydrogen repartition in this SSY configuration, using the ADVENTURE finite element software [22]. They assumed that the McNabb and Foster equation could be used in conjunction with the "strain rate factor" in the context of trap creation. Their conclusions pointed out that Oriani's assumption is not suitable for fast loadings. They showed important differences with the Krom et al.'s results, and suggested the potential interest of transient trapping for HELP model.

Recently, another implementation of the McNabb and Foster equation, in the commercial Finite Element software Abaqus© based on User Subroutines [23], has been proposed [24], in order to solve various coupled mechanical-diffusion and transient trapping problems. Such an implementation is indeed challenging: ~~i~~n Abaqus©, it is needed, for the sake of global convergence, that the User Subroutines provide to the software the temporal evolution of several partial derivatives (see [15] for details). These partial derivatives have been evaluated by Benannoune et al. [24] using an approximation of the solution of the McNabb and Foster differential equation (see below equation (3)). This approach was used to solve initial boundary values problems involving transient hydrogen trapping processes, either without trap creation (e.g., on Thermal Desorption Spectroscopy spectrums), or for more complex problems, in which hydrogen diffusion, and transient trapping have been coupled with evolving (thermo)mechanical fields [25-28].

The present study aims at extending the work of Krom et al. [2] to transient trapping by improving the formulation proposed by Kanayama et al.. Oriani's assumption and the strain rate factor correction, are replaced by the original McNabb and Foster relationship, as it is done in several studies related to plasma-surface interactions (see, e.g., [29-31]).

First the main hydrogen transport equations are described. Then the issues induced by the Kanayama et al. approach are pointed out, in the case of an insulated body under a uniform mechanical load. A reformulation of the used equations is then proposed and, for the sake of comparison with previous work, a parametric study on the SSY test case used by Krom et al. is conducted for bcc iron. Only trapping by dislocations is considered here but the approach could be adapted to other kind of traps.

All computations have been made using Abaqus Software and User Subroutines (details can be found in [24,32,33]).

2 Hydrogen transport and trapping evolution

2.1 Hydrogen transport equation

The hydrogen concentration in the bulk C is assumed to be the sum of the diffusive hydrogen concentration C_L and of the trapped hydrogen concentration C_T. Only one kind of trap is considered, i.e., dislocation core, which is saturable and reversible. The hydrogen concentrations are related to the number of sites: $C_L = \theta_L N_L$, where θ_L is the occupancy of the lattice sites and N_L the number of lattice sites per unit volume, and $C_T = \theta_T N_T$, where θ_T is the occupancy of the lattice sites and N_T the number of lattice sites per unit volume.

Considering the effect of a hydrostatic stress on the chemical potential of the hydrogen in the lattice sites, the hydrogen flux is [1]

$$\boldsymbol{\varphi} = -D_L \boldsymbol{\nabla} C_L - D_L C_L \frac{V_H}{RT} \boldsymbol{\nabla} P_H \tag{1}$$

where $P_H = -\sum \sigma_{ii}/3$ is the hydrostatic pressure, V_H the partial molar volume of hydrogen, D_L the hydrogen diffusion coefficient, T the absolute temperature and R the universal gas constant. From mass conservation, the changing rate of the total hydrogen concentration C inside an arbitrary volume is equivalent to the flux through its external surface, leading to

$$\frac{\partial C_L}{\partial t} + \frac{\partial C_T}{\partial t} = \boldsymbol{\nabla}.\left(D_L \boldsymbol{\nabla} C_L + D_L C_L \frac{V_H}{RT} \boldsymbol{\nabla} P_H \right) \tag{2}$$

The main differences in the different approaches that can be found in the literature are related to the formulation of $\partial C_T/\partial t$. The various expressions of this rate encountered in the literature are presented and discussed below.

2.2 Expressions of the trapped hydrogen concentration rate

McNabb and Foster [7] assumed the trapping process can be summarized by the following chemical reaction [34]

$$C_L + N_T^* \leftrightharpoons C_T + N_L^* \tag{3}$$

where N_T^* and N_L^* are respectively the free trapping sites and the free lattice sites densities ($N_T = C_T + N_T^*$). Assuming a first order chemical reaction, this leads to

$$\frac{\partial C_T}{\partial t} = \frac{k}{N_L} C_L N_T^* - \frac{p}{N_L} C_T N_L^* \tag{4}$$

where k/N_L and p/N_L are the forward and reverse reaction rates constants. If $N_L \gg C_L$ (i.e., $N_L \approx N_L^*$, or $\theta_L \ll 1$, which is a common approximation in the context of plasticity) equation (4) can be simplified as following

$$\frac{\partial C_T}{\partial t} = \frac{k}{N_L} C_L (N_T - C_T) - p C_T \tag{5}$$

Moreover, McNabb and Foster [7] assumed a constant trap density N_T, so that equation (5) naturally implies

$$\frac{\partial \theta_T}{\partial t} = k \theta_L (1 - \theta_T) - p \theta_T \tag{6}$$

The steady state solution of equation (6), as proposed by Oriani [9], is written as

$$K_T \theta_L = \frac{\theta_T}{1 - \theta_T} \tag{7}$$

where K_T is the equilibrium constant for equation (6), so that $K_T = e^{-\Delta E_T/RT}$ with ΔE_T the trap binding energy with respect to the lattice site, R the universal gas constant and T the absolute temperature. K_T is linked to the rate constants by $K_T = k/p$.

At equilibrium, equation (7) therefore gives an explicit relation between θ_T and θ_L. Assuming that N_T only depends on the equivalent plastic stain $\bar{\varepsilon}_p$ [2], the evolution of the trapped hydrogen concentration can be written as

$$\frac{\partial C_T}{\partial t} = N_T \frac{\partial \theta_T}{\partial t} + \theta_T \frac{dN_T}{dt} = N_T \frac{\theta_T(1-\theta_T)}{\theta_L} \frac{\partial \theta_L}{\partial t} + \theta_T \frac{dN_T}{d\bar{\varepsilon}_p} \dot{\bar{\varepsilon}}_p \quad (8)$$

in which $\partial\theta_T/\partial t$ is computed from equation (7). The last term of equation (8), the "strain rate factor", was added to the initial approach [1] due to the lack of hydrogen balance pointed out when considering an insulated, uniformly stressed body (see section 3 below).

To account for transient trapping, Kanayama et al. [16] used the expression of $\partial\theta_T/\partial t$ given by equation (6), leading to

$$\frac{\partial C_T}{\partial t} = N_T \frac{\partial \theta_T}{\partial t} + \theta_T \frac{dN_T}{dt} = N_T[k\theta_L(1-\theta_T) - p\theta_T] + \theta_T \frac{dN_T}{d\bar{\varepsilon}_p} \dot{\bar{\varepsilon}}_p \quad (9)$$

Kanayama et al. showed that this formulation produces drastically different hydrogen distribution when compared to the use of Oriani's equilibrium theory, particularly when the loading time is significantly small (or the strain rate is high). Their approach has been used in several recent works [16,24-28].

However, the assumption of a constant trap density in equation (6) appears to be problematic considering the evolution of trap density with plastic strain used in equation (8). The current study therefore proposes to directly use equation (5) in the transport equation (2) to account for transient trapping in finite element simulations of diffusion problems. As a consequence, the "strain rate factor" is no longer needed and the hydrogen transport equation reads

$$\frac{\partial C_L}{\partial t} + k\theta_L\left(N_T(\bar{\varepsilon}_p) - C_T\right) - pC_T = \boldsymbol{\nabla}.\left(D_L \boldsymbol{\nabla} C_L + D_L C_L \frac{V_H}{RT} \boldsymbol{\nabla} P_H\right) \quad (10)$$

In the next section, the relevance of this new formulation is first analyzed in the case of an insulated, uniformly-stressed body, following [2].

A comparison with literature results obtained on the SSY benchmark test case [1,2] is then conducted.

The influence of the trapping kinetic is then focused on by conducting a parametric study on the reaction rate constants p and k, with $k/p=K_T$ set as a constant (linked to the dislocation binding energy, for the sake of comparison). This allows going through any trapping configuration, from an almost purely diffusive process (with a very slow trapping, when $p \to 0^+$ s^{-1}) to instantaneous trapping (consistent with the Oriani's assumption, when $p \to +\infty$ s^{-1}).

3 Diffusive and trapped hydrogen concentration in the case of an insulated, uniformly-stressed body

3.1 Modeling assumptions

The configuration and assumptions used by Krom et al. (justifying the "(plastic) strain rate factor" [2]) are used in this section. The objective is to compare the results obtained with equations (8), (9) and (10).

A bar made of α-iron is considered. It is assumed to be insulated (i.e., no hydrogen normal flux on the outer bar surfaces). At $t = 0$, $C_L = C_0$ and $C_T = 0$, with C_0=2.08×10^{21} m^{-3} [1].

This bar is mechanically loaded with a constant displacement rate (set equal to 0.01 mm/s^{-1}), leading to plastic strain increase, and thus, dislocation-related trap creation. As each field is uniform in the bar, the diffusive hydrogen flux is zero everywhere ($\boldsymbol{\varphi}$ =**0**) and the total hydrogen concentration is therefore constant ($C_L + C_T = C_0$).

The elastic-plastic behavior is described by

$$\varepsilon = \begin{cases} \dfrac{\sigma}{E} \; if \; \varepsilon \leq \dfrac{\sigma_Y}{E} \\ \dfrac{\sigma_Y}{E}\left(\dfrac{\sigma}{\sigma_Y}\right)^n \; if \; \varepsilon \geq \dfrac{\sigma_Y}{E} \end{cases} \tag{11}$$

where E is the Young modulus and σ_Y the yield stress. The evolution of the trap density with the plastic strain is expressed by [1,35] (N_T in m^{-3})

$$\log N_T = 23.26 - 2.33e^{-5.5\bar{\varepsilon}_p} \tag{12}$$

p is set to 0.001 s^{-1}, and $k = K_T \times p$. The used parameters are enlisted in Table 1.

Table 1. Parameters for α-iron at room temperature (from [1,2]).

D_L (m^2/s)	V_H (m^3)	N_L (m^{-3})	ΔE_T (kJ)	E (GPa)	ν	σ_Y (MPa)	n
1.27×10^{-8}	2×10^{-6}	5.1×10^{29}	60	207	0.3	250	5

3.2 Results

The comparison of the evolution of the diffuse and trapped hydrogen concentrations with plastic strain when using equations (8) or (9) is presented on Figure 1.

When equation (8) is used (dashed lines), the simulation reproduces the results of Krom et al. [2]: when the plastic strain increases, traps are created modifying the balance between C_L and C_T to the advantage of the latter. At higher values of plastic strain ($\bar{\varepsilon}_p > 0.04$), there is almost no mobile particles left in the sample.

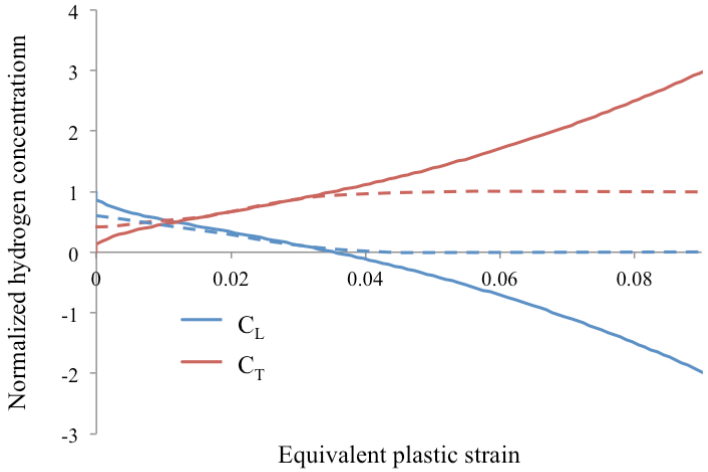

Figure 1. Effect of the use of equation (9) –Kanayama et al. [16], full lines- on the evolution of hydrogen concentrations with plastic strain, compared with the Krom et al. results [2] based on equation (8) –Krom et al. [2], dashed lines-.

Compared with the case of instantaneous trapping based on equation (8), the use of equation (9) leads to significantly lower C_T values for low plastic strains, which is not surprising. But what is evident on Figure 1 is that C_L becomes negative after a few percents plastic strain, which is not physical, while C_T becomes greater than C_0. This is explained as follow.

In the present configuration, as the total hydrogen concentration remains constant, equation (9) leads to

$$\frac{\partial C_L}{\partial t} = -N_T[k\theta_L(1-\theta_T) - p\theta_T] - \theta_T \frac{dN_T}{d\bar{\varepsilon}_p}\dot{\bar{\varepsilon}}_p \quad (13)$$

In equation (13), $\dot{\bar{\varepsilon}}_p > 0$ (due to the loading configuration), inducing an increase of the trap density ($dN_T/d\bar{\varepsilon}_p > 0$). This increase favors hydrogen trapping over detrapping, i.e. $k\theta_L(1-\theta_T) - p\theta_T > 0$. As a consequence, $\partial C_L/\partial t < 0$ when plastic strain increase, leading, at some point, to negative C_L values. It is worth underlining that, in previous works based on equation (9) [16,24-28], no negative C_L values have been detected, mainly because total hydrogen concentration was not constant with time.

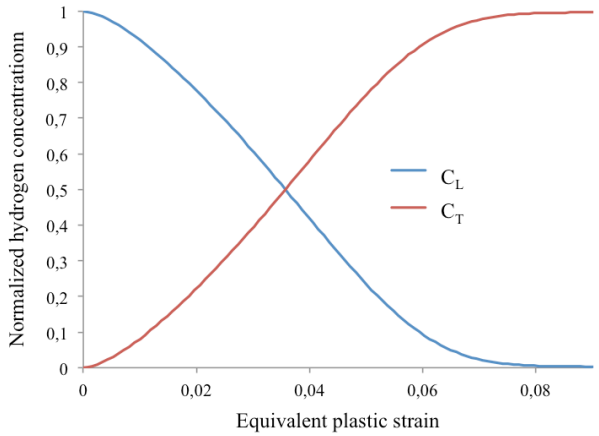

Figure 2. Effect of the use of equation (10) on the concentration evolution with plastic strain.

On the contrary, when using equation (10), consistent evolutions of the hydrogen concentrations are obtained as it can be seen on Figure 2: C_L and C_T are bounded by 0 and C_0 and their variations remain physically consistent. As a consequence Equation (10) appears more relevant to describe hydrogen transient transport than equation (9) and is considered in the next sections, focusing on the effect of transient trapping on the hydrogen concentration evolution in the reference SSY configuration.

4 Application and parametric study

4.1 SSY configuration

The considered SSY geometry of the reference configurations [1,2] is presented on Figure 3. The main features are described below.

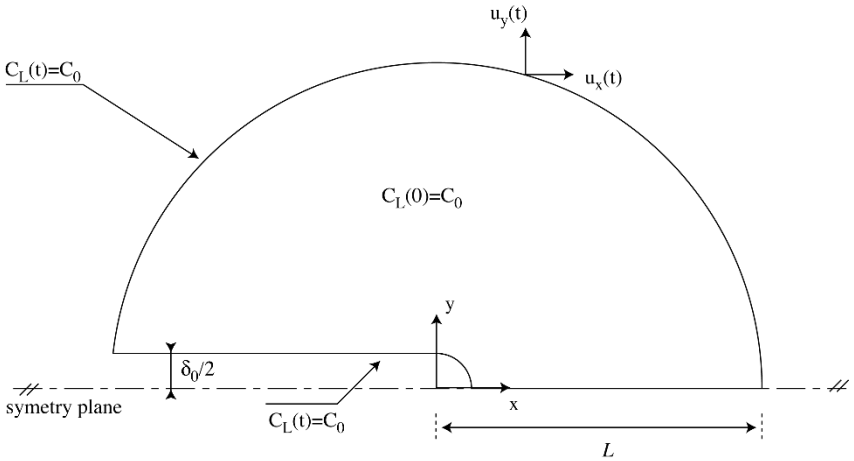

Figure 3. Geometrical configuration and boundary conditions of the SSY problem.

δ_0 is set to 10 µm, L to 150 mm.

Symmetry boundary conditions on the crack path are imposed for both the diffusive and mechanical fields. Displacements are imposed on the outer boundary. They are known from the elastic solution, which is controlled by the mode I stress intensity factor K_I, with [36]

$$\begin{cases} u_x = \dfrac{(1+\nu)K_I}{E}\sqrt{\dfrac{r}{2\pi}}\cos\dfrac{\theta}{2}\left(\kappa - 1 + 2\sin^2\dfrac{\theta}{2}\right) \\ u_y = \dfrac{(1+\nu)K_I}{E}\sqrt{\dfrac{r}{2\pi}}\sin\dfrac{\theta}{2}\left(\kappa + 1 - 2\cos^2\dfrac{\theta}{2}\right) \end{cases} \tag{14}$$

with $\kappa = 3 - 4\nu$. r and θ are the polar coordinates of the current point. Each simulation is controlled by the rate $\dot{K}_I = K_I/T$, for a mechanical loading up to the prescribed K_I value for a given loading duration T. $C_L = C_0$ is imposed on the crack surfaces and the outer boundary.

At $t = 0$, there is no mechanical loading; C_L is set to C_0 in the sample, while $C_T(t = 0)$ is computed using the Oriani's relationship (equation (7)), considering the trap density $N_T(\bar{\varepsilon}_p = 0)$.

Parameters given in section 3.1 are used thereafter, unless specified.

The reference case is taken from [2], with $K_I = 89.2$ MP$a\sqrt{m}$ and T=130 s (leading to $\dot{K}_I = 0.68$ MP$a\sqrt{m}$/s for $t \in [0, T]$). For $t \in [T, 1419\ h]$, the mechanical loading remains constant ($\dot{K}_I = 0$ MP$a\sqrt{m}$/s). The p value is set to 0.001 s^{-1} ($k = K_T \times p$): it has been checked that these reaction rate constants values allows to get an instantaneous trapping in the reference case (see Figure 5a or Figure 6 below).

The modeling assumptions are first validated on the reference case.

Then, a parametric study on the time T is conducted, and compared with the results obtained by Krom et al., to point out the differences resulting from the transient trapping assumption. Following [2], two boundary conditions on the crack are considered: insulated or $C_L = C_0$.

In the last section, the influence of the reaction rate constants (k, p) on the results is investigated for two T values.

4.2 Comparison with the reference case

For the sake of comparison, the stress triaxality variation with the distance ahead of the crack tip is plotted on Figure 4. The distance from the crack tip r is normalized by b, which is the crack opening displacement, and $b/b_0 = 4.7$. It can be observed that the mechanical fields are in a very good agreement with the one from Krom at al., i.e., a little bit lower than the

Sofronis and McMeeking ones. It is pointed out in [2] that such a difference can be due to differences in the mechanical behavior formulation, based on Kirchhoff stresses in the Sofronis and McMeeking study, whereas Cauchy stresses are used in [2] and in the present study.

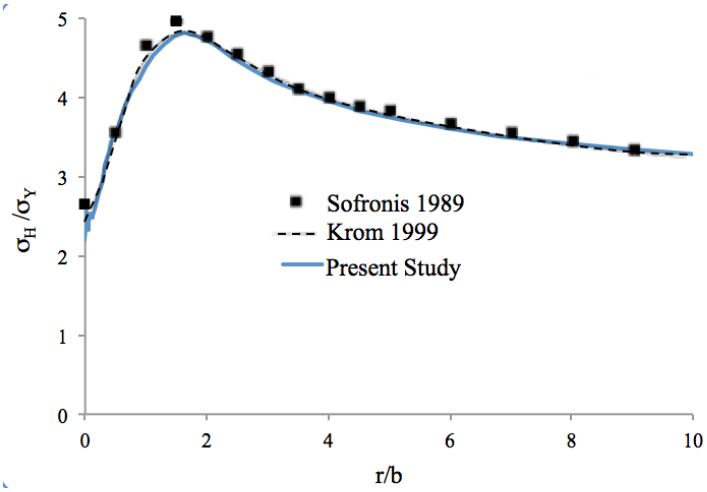

Figure 4. Comparison of the stress triaxialities σ_H/σ_Y, where $\sigma_H = \sum\sigma_{ii}/3$, at the end of the mechanical loading ($t = T$=130 s) in the front of the crack tip ($\theta = 0$) as computed by Sofronis and McMeeking [1], Krom et al. [2] and in the present study.

Diffusive hydrogen repartition along the crack path ($\theta = 0$) is plotted on Figure 5a.

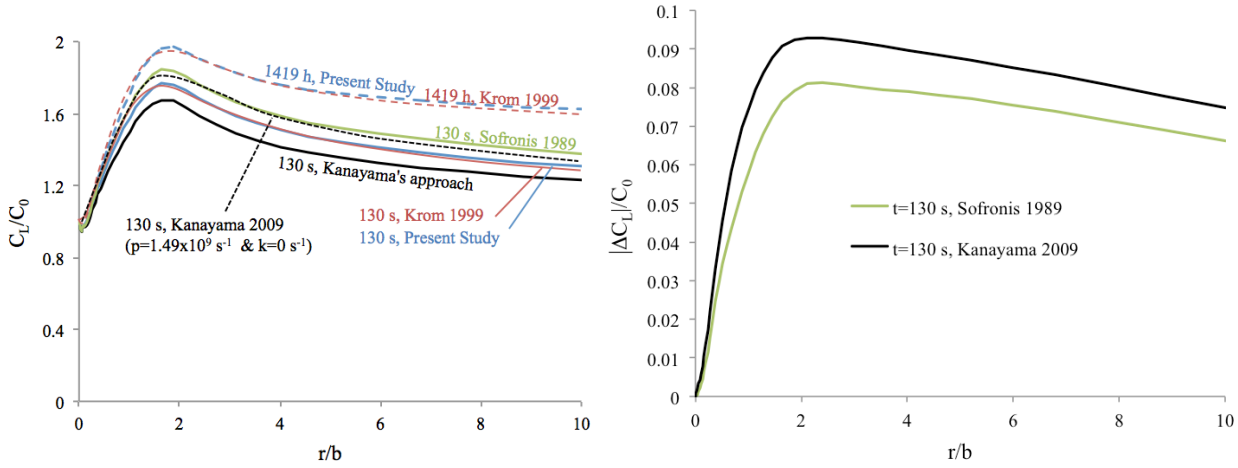

(a) (b)

Figure 5. (a) C_L evolution along the crack path ($\theta = 0$) at the end of the mechanical loading (T=130 s) and at the end of the simulation (1419 h) as computed by Sofronis and McMeeking [1], Krom et al. [2], using Kanayama's approach [16], and in the present study. (b) Comparaison of the differences induced by the Sofronis and McMeeking and Kanayama et al. approaches on the C_L values along the crack path (the reference being the Krom et al. results: $\Delta C_L = C_L - C_L^{Krom\ et\ al.}$).

As seen on Figure 4 and on Figure 5a, equation (10) allows to get a very good reproduction of the results from Krom et al. based on equation (8), as soon as (i) the reaction rate constants values are consistent with an instantaneous trapping and (ii) the same kind of trap is considered ($k = K_T \times p$, with $K_T = e^{-\Delta E_T/RT}$).

Figure 5a also shows the differences at $t = T$ =130 s with the results obtained by Sofronis and McMeeking, which overestimate the C_L repartition; as explained by Krom et al., this is because trap creation is not accounted for. Using Kanayama et al. approach, C_L repartition is

underestimated, as illustrated on Figure 5b; in this case, it can be argued that the trap creation is accounted for twice (in the McNabb and Foster equation, and in the strain rate factor).

It is worth noting that this latter C_L repartition is not the one shown in [16] (black dashed line in Figure 5a) for it corresponds to another trapping equilibrium condition: in [16] Kanayama et al. have used k=1.49×10^9 s^{-1} and $p = 0\ \mathrm{s}^{-1}$, i.e., $k \neq K_T \times p$. Therefore their results cannot be directly compared with [5,6].

4.3 Influence of the loading time

Two boundary conditions are investigated, differing by the C_L value on the crack (respectively $C_L = C_0$ and insulated). Several loading times T have been considered, following [2]: 1.3 s, 3.25 s, 6.5 s, 13 s and 130 s for the $C_L = C_0$ boundary condition, and 1.3 s,13 s, 26 s, 130 s, 1300 s and 1300000 s for the insulated configuration.

The evolutions of the normalized C_L repartition at the end of the mechanical loading ($t = T$) along the crack path are plotted on Figure 6 for the first boundary condition ($C_L = C_0$), and on Figure 7 for the condition of insulation.

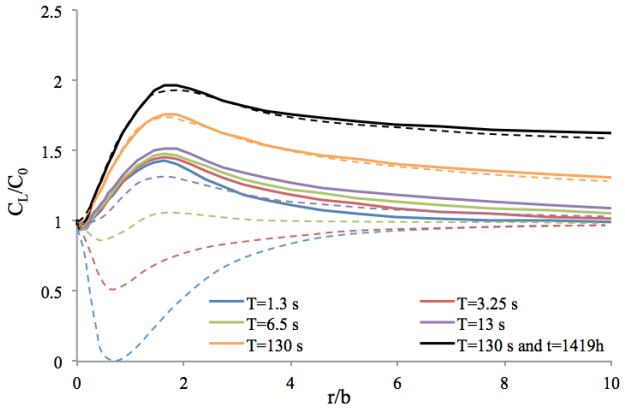

Figure 6. Comparison of the normalized diffusive hydrogen concentration along the crack path at the end of the mechanical loading for several T values. T=130 s corresponds to the reference configuration. For the sake of comparison, results obtained by [2] have been also plotted (dashed line). Unless specified, the curves are plotted at $t = T$.

The impact of a transient trapping model on C_L distribution appears to be more salient when the loading time T decreases, i.e., when the trapping process is out of equilibrium (reached for a loading time T larger than 130 s).

Upon the assumption of instantaneous trapping, trap creation acts as a "sink" for C_L, and therefore its decrease is less and less compensated by the diffusion process when T decreases.

The above results illustrate the competition between the mechanical loading characteristic time and the trapping one. When the loading time is significantly longer than the trapping time the instantaneous trapping assumption is relevant.

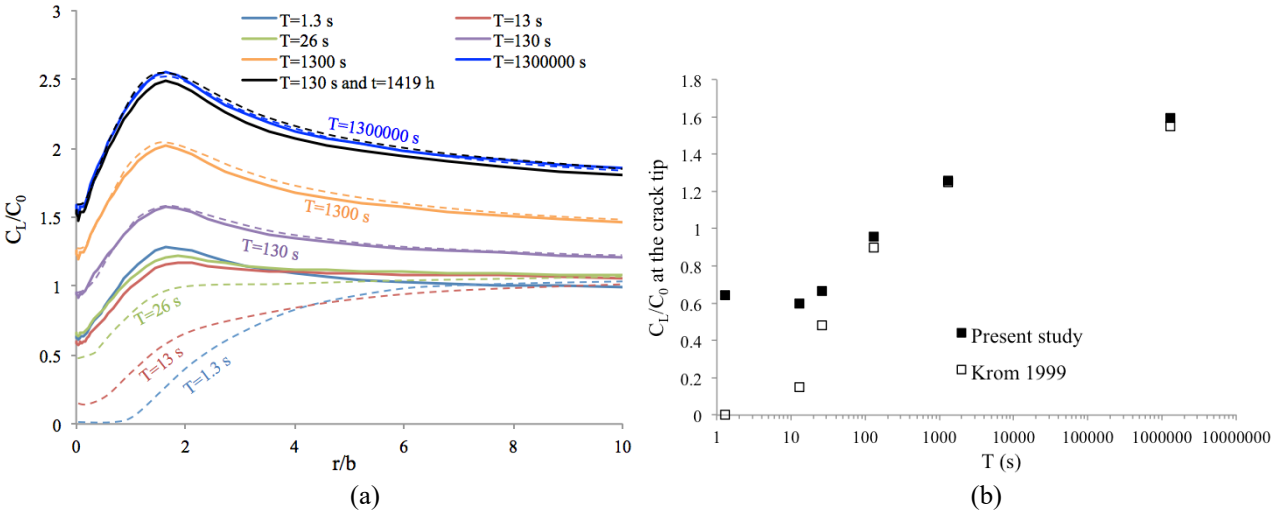

(a) (b)

Figure 7. (a) Evolution of the normalized diffusive hydrogen concentration along the crack path at the end of the mechancial loading for several T values and (b) value of C_L/C_0 at the insulated crack tip. Values computed by Krom are plotted the the sake of comparison (dashed lines).

The same tendencies can be observed when considering the insulated crack configuration (Figure 7a), in which differences between the Krom et al. approach and the present study appear also important. From the superposition of the curves for $T \geq 130$ s, it is confirmed that p=0.001 s^{-1} is high enough to get an instantaneous trapping process; this is not the case for lower T values, as in Figure 6.

For $T \geq 130$ s, the increase of C_L with T at the crack tip indicates hydrogen supply from the outer surfaces (Figure 7b).

For both configurations, the impact of a transient trapping approach appears to be more important when the loading time decreases, i.e, when the trapping process can not reach its steady state. In other words, if the chosen reaction rate constants lead to an instantaneous trapping for $T \geq 130$ s, for lower T values, this is no longer the case, echoing Kayanama's conclusion on the Oriani's domain of validity adapted to "long" loading times.

Obviously, the value of T at which the trapping could be considered as instantaneous depends on the chosen values for the reaction rate constants. This point is focused on thereafter, for T=130 and 1.3 s and several (k, p) values.

4.4 Influence of the reaction rate constants

To analyze in more detail the influence of the transient trapping, the influence of the trapping kinetics is focused on; as in the previous sections, only the p parameter is set as a variable for the reference configuration, $K_T = e^{-\Delta E_T/RT}$ being kept constant and k set to $K_T \times p$.

The evolution of C_L and C_T along the crack path at the end of the mechanical loading ($t = T$) is plotted on Figure 8 and Figure 9, for T=130 s and 1.3 s, respectively.

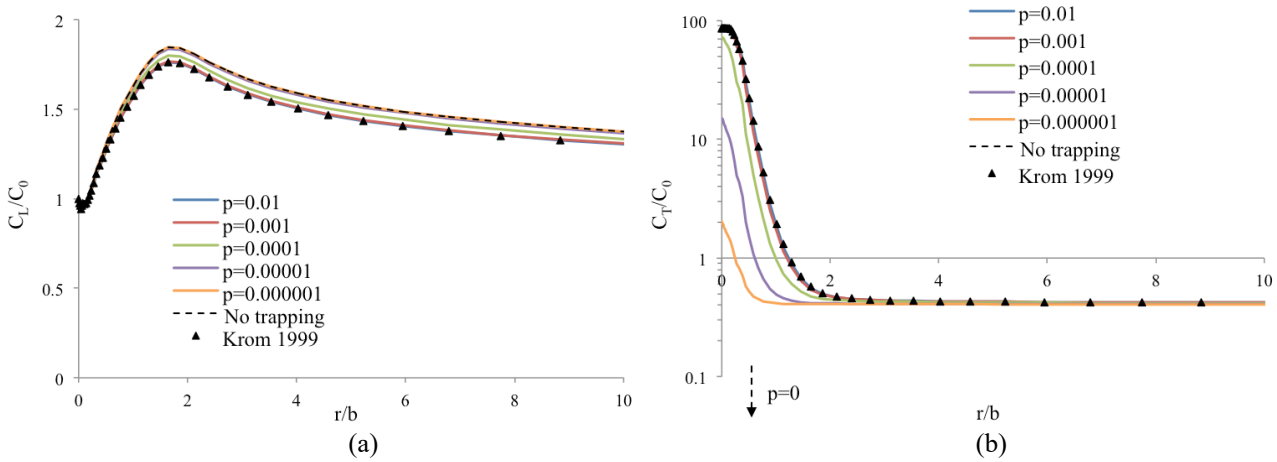

Figure 8. Evolution of the normalized (a) diffusive and (trapped) concentration along the crack path for the reference at $t = T$=130 s for different value of p (while keeping K_T constant), in s^{-1}. 'No trapping' corresponds to p=0 s^{-1}.

It can be seen that all C_L curves spread between the two extreme configurations, i.e., instantaneous trapping (Krom et al. approach, corresponding to high p values – here, greater to 0.001 s^{-1}), and trapping-free (for low p values – here, lower to 0.000001 s^{-1}). The C_L values increase with a decreasing p, while the C_T ones decrease. As seen on Figure 8b, if C_L repartition is consistent with a trapping-free approach for $p \leq$0.000001 s^{-1}, this is not the case for the C_T repartition, which exhibits a slight increase near the crack tip. Close to the crack tip, the p value has no influence on the diffusive hydrogen concentration distribution due to the boundary condition on C_L.

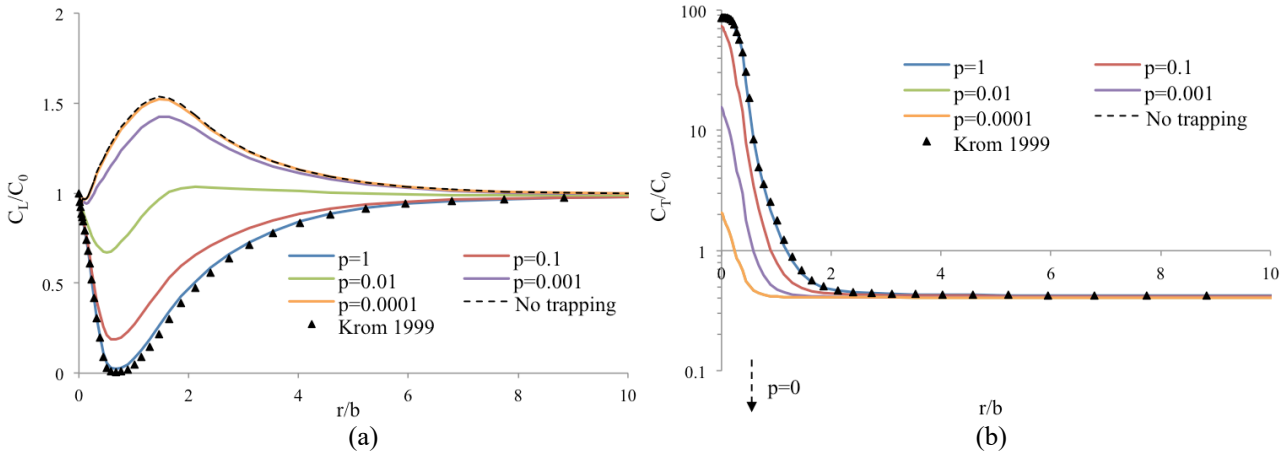

Figure 9. Evolution of the normalized (a) diffusive and (trapped) concentration along the crack path for the reference case at $t = T$=1.3 s for different value of p (while keeping K_T constant), in s^{-1}. 'No trapping' corresponds to p=0 s^{-1}.

For T=1.3 s, the previous conclusions are still valid, provided adapted p values: $p \geq$1 s^{-1} corresponds to an instantaneous trapping, and is $p \leq$0.0001 s^{-1} to a trapping-free diffusion.

On Figure 10 are plotted the evolution of the total hydrogen along the crack path for different values of p, for t=T=130 and 1.3 s.

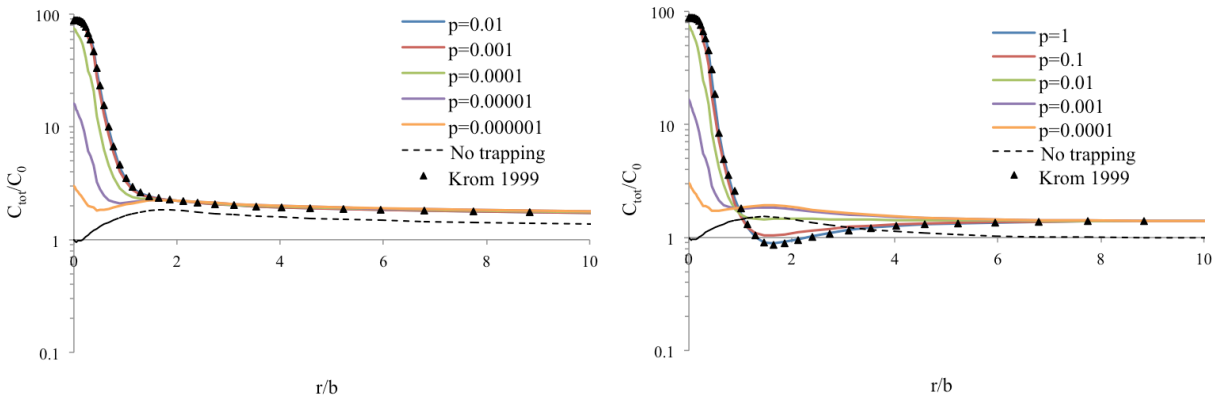

Figure 10. Evolution of the normalized total hydorgen concentration $C_{tot} = C_L + C_T$ for (a) $t = T$=130 s and (b) $t = T$=1.3 s for different value of p (while keeping K_T constant), in s^{-1}. 'No trapping' corresponds to p=0 s^{-1}.

At the crack tip, differences with the results from Krom et al. are here very important. For $t = T$=130 s, instantaneous trapping assumption leads to an upper bound value for C_{tot}. For $t = T$=1.3 s, the C_{tot} repartition evolution with p is more complex. The depletion at $r/b \approx 1$ is connected to that of C_L(see Figure 9a), denoting the "sinking" due to trap creation which increases when p decreases and is maximum for instantaneous trapping.

Such a depletion is not seen at T=130 s, for diffusion characteristic time is sufficient to compensate "sinking" by trapping.

Conclusion

In this study, different formulations of a hydrogen transport model assisted by mechanical fields are compared for a reference SSY configuration, focusing on the more relevant introduction of transient trapping in the equations of the literature used for solving initial boundary values problems by finite element simulations.

Due to the assumption of instantaneous trapping under Oriani equilibrium, the hydrogen transport equation proposed by Krom et al. [2], whose improved formulation of the previous model of Sofronis and McMeecking [1] by the introduction of a "strain rate factor" in case of trap creation, appears to be non suitable to simultaneously account for trap density variation and transient trapping, as non-physical hydrogen concentrations values can be obtained in a specific test configuration. Alternatively, numerical simulations based on the reformulation of the equations from the original McNabb and Foster kinetic trapping equation, describing a first order chemical reaction including implicitly trap creation show, in this case, consistent results and demonstrate that this approach is more relevant.

The numerical simulations of the reference SSY configuration conducted with this new formulation show that accounting for a transient trapping phenomenon can lead to significant differences in diffusive and trapped hydrogen concentrations values ahead of a crack tip, depending on the competition between trap creation -i.e., here, plasticity-, and trapping. The numerical sensitivity analysis has also estimated for the considered trap binding energy the range of the reaction rate constants values consistent with the Oriani's domain of validity.

More generally, the present work shows the importance of checking the relevance of transient trapping as this could have a great influence on the prediction of the models of embrittlement and crack propagation triggered or assisted by hydrogen.

Acknowledgements

This work has been carried out within the framework of the EUROfusion Consortium and has received funding from the Euratom research and training programme 2014-2018 and 2019-2020 under grant agreement No 633053. The views and opinions expressed herein do not necessarily reflect those of the European Commission.

The authors thank R. Delaporte-Mathurin for his help in improving the article.

Bibliography

[1] Sofronis P, McMeeking RM. Numerical analysis of hydrogen transport near a blunting crack tip. J Mech Phys Solids 1989;37:317–50. doi:10.1016/0022-5096(89)90002-1.

[2] Krom AHM, Koers RWJ, Bakker AD. Hydrogen transport near a blunting crack tip. J Mech Phys Solids 1999;47:971–92. doi:10.1016/S0022-5096(98)00064-7.

[3] Dwivedi SK, Vishwakarma M. Hydrogen embrittlement in different materials: A review. Int J Hydrog Energy 2018;43:21603–16. doi:10.1016/j.ijhydene.2018.09.201.

[4] Djukic MB, Bakic GM, Sijacki Zeravcic V, Sedmak A, Rajicic B. The synergistic action and interplay of hydrogen embrittlement mechanisms in steels and iron: Localized plasticity and decohesion. Eng Frac Mech 2019:106528. doi:j.engfracmech.2019.106528.

[5] Depover T, Hajilou T, Wan D, Wang D, Barnoush A, Verbeken K. Assessment of the potential of hydrogen plasma charging as compared to conventional electrochemical hydrogen charging on dual phase steel. Mater Sci Eng A 2019;754:613–21. doi:10.1016/j.msea.2019.03.097.

[6] Quirós C, Mougenot J, Lombardi G, Redolfi M, Brinza O, Charles Y, et al. Blister formation and hydrogen retention in aluminium and beryllium: A modeling and experimental approach. Nucl Mat Ener 2017;12:1178–83. doi:10.1016/j.nme.2016.12.036.

[7] McNabb A, Foster PK. A new analysis of the diffusion of hydrogen in iron and ferritic steels. Trans Metall Soc AIME 1963;227:618–27.

[8] Espenson JH. Chemical Kinetics and Reaction Mechanisms. McGraw-Hill; 1995.

[9] Oriani RA. The diffusion and trapping of hydrogen in steel 1970;18:147–57. doi:10.1016/0001-6160(70)90078-7.

[10] Taha A, Sofronis P. A micromechanics approach to the study of hydrogen transport and embrittlement. Eng Frac Mech 2001;68:803–37. doi:http://dx.doi.org/10.1016/S0013-7944(00)00126-0.

[11] Liang Y, Sofronis P, Dodds RH Jr. Interaction of hydrogen with crack-tip plasticity: effects of constraint on void growth. Mater Sci Eng A 2004;366:397–411. doi:10.1016/j.msea.2003.09.052.

[12] Dadfarnia M, Sofronis P, Neeraj T. Hydrogen interaction with multiple traps: Can it be used to mitigate embrittlement? Int J Hydrog Energy 2011;36:10141–8. doi:10.1016/j.ijhydene.2011.05.027.

[13] Martínez-Pañeda E, del Busto S, Niordson CF, Betegón C. Strain gradient plasticity modeling of hydrogen diffusion to the crack tip. Int J Hydrog Energy 2016;41:10265–74. doi:10.1016/j.ijhydene.2016.05.014.

[14] Dadfarnia M, Martin ML, Nagao A, Sofronis P, Robertson IM. Modeling hydrogen transport by dislocations. J Mech Phys Solids 2015;78:511–25. doi:10.1016/j.jmps.2015.03.002.

[15] Oh C-S, Kim YJ, Yoon KB. Coupled analysis of hydrogen transport using ABAQUS. J Solid Mech Mater Eng 2010;4:908–17. doi:10.1299/jmmp.4.908.
[16] Kanayama H, Ndong-Mefane S, Ogino M, Miresmaeili R. Reconsideration of the Hydrogen Diffusion Model Using the McNabb-Foster Formulation. Mem Fac Eng Kyushu Univ 2009;69:146–61.
[17] Martínez-Pañeda E, Díaz A, Wright L, Turnbull A. Generalised boundary conditions for hydrogen transport at crack tips. Corros Sci 2020:108698. doi:10.1016/j.corsci.2020.108698.
[18] Jemblie L, Olden V, Akselsen OM. A coupled diffusion and cohesive zone modelling approach for numerically assessing hydrogen embrittlement of steel structures. Int J Hydrog Energy 2017;42:11980–95. doi:10.1016/j.ijhydene.2017.02.211.
[19] Anand L, Mao Y, Talamini B. On modeling fracture of ferritic steels due to hydrogen embrittlement. J Mech Phys Solids 2019;122:280–314. doi:10.1016/j.jmps.2018.09.012.
[20] Charles Y, Nguyen TH, Ardon K, Gaspérini M. Scale Transition in Finite Element Simulations of Hydrogen–Plasticity Interactions. In: Ionescu I, Queyreau S, Picu C, Salman OU, editors. Mechanics and Physics of Solids at Micro- and Nano-Scales. 1st ed., Wiley; 2019, pp. 87–129. doi:10.1002/9781119687566.ch4.
[21] Kumar R, Mahajan DK. Hydrogen distribution in metallic polycrystals with deformation. J Mech Phys Solids 2020;135:103776. doi:10.1016/j.jmps.2019.103776.
[22] Yoshimura S, Shioya R, Noguchi H, Miyamura T. Advanced general-purpose computational mechanics system for large-scale analysis and design. J Comput Appl Math 2002;149:279–96.
[23] Simulia. Abaqus User subroutines reference guide. Dassault Système; 2011.
[24] Benannoune S, Charles Y, Mougenot J, Gaspérini M. Numerical simulation of the transient hydrogen trapping process using an analytical approximation of the McNabb and Foster equation. Int J Hydrog Energy 2018;43:9083–93. doi:10.1016/j.ijhydene.2018.03.179.
[25] Benannoune S, Charles Y, Mougenot J, Gaspérini M, De Temmerman G. Numerical simulation by finite element modelling of diffusion and transient hydrogen trapping processes in plasma facing components. Nucl Mat Ener 2019;19:42–6. doi:10.1016/j.nme.2019.01.023.
[26] Charles Y, Gaspérini M, Fagnon N, Ardon K, Duhamel A. Finite element simulation of hydrogen transport during plastic bulging of iron submitted to gaseous hydrogen pressure. Eng Frac Mech 2019;218:106580. doi:10.1016/j.engfracmech.2019.106580.
[27] Díaz A, Alegre JM, Cuesta II, Zhang Z. Numerical study of hydrogen influence on void growth at low triaxialities considering transient effects. Int J Mech Sci 2019;164:105176. doi:10.1016/j.ijmecsci.2019.105176.
[28] Benannoune S, Charles Y, Mougenot J, Gaspérini M, De Temmerman G. Multidimensional finite-element simulations of the diffusion and trapping of hydrogen in plasma-facing components including thermal expansion. Phys Scr 2020;T171:014011. doi:10.1088/1402-4896/ab4335.
[29] Bonnin X, Hodille EA, Ning N, Sang C, Grisolia C. Rate equations modeling for hydrogen inventory studies during a real tokamak material thermal cycle. J Nucl Mater 2015;463:970–3. doi:10.1016/j.jnucmat.2014.10.053.
[30] Hodille EA, Bonnin X, Bisson R, Angot T, Becquart CS, Layet JM, et al. Macroscopic rate equation modeling of trapping/detrapping of hydrogen isotopes in tungsten materials. J Nucl Mater 2015;467:424–31. doi:10.1016/j.jnucmat.2015.06.041.
[31] Delaporte-Mathurin R, Hodille EA, Mougenot J, Charles Y, Grisolia C. Finite

element analysis of hydrogen retention in ITER plasma facing components using FESTIM. Nucl Mat Ener 2019;21:100709. doi:10.1016/j.nme.2019.100709.
[32] Charles Y, Nguyen TH, Gaspérini M. FE simulation of the influence of plastic strain on hydrogen distribution during an U-bend test. Int J Mech Sci 2017;120:214–24. doi:10.1016/j.ijmecsci.2016.11.017.
[33] Charles Y, Nguyen TH, Gaspérini M. Comparison of hydrogen transport through pre-deformed synthetic polycrystals and homogeneous samples by finite element analysis. Int J Hydrog Energy 2017;42:20336–50. doi:10.1016/j.ijhydene.2017.06.016.
[34] Drexler A, Depover T, Leitner S, Verbeken K, Ecker W. Microstructural based hydrogen diffusion and trapping models applied to Fe–CX alloys. J Alloy Compd 2020;826:154057. doi:10.1016/j.jallcom.2020.154057.
[35] Kumnick AJ, Johnson HH. Deep trapping states for hydrogen in deformed iron 1980;28:33–9. doi:10.1016/0001-6160(80)90038-3.
[36] Rice JR. Mathematical analysis in the mechanics of fracture. In: Liebowitz H, editor. Fracture: An Advanced Treatise, vol. 2, Fracture: an advanced treatise; 1968, pp. 191–311.